

System Identification and Experimental Modal Analysis of a Frame Structure

Carmin Maria Pappalardo, Domenico Guida

Abstract—In this paper, an effective method for performing the experimental modal analysis of structural systems is developed. The proposed methodology is corroborated by analytical considerations and is verified experimentally. The identification method developed in this paper is based on time-domain system identification numerical techniques. The case study considered in this work is a frame structure that can be modeled as a two-story shear building system. A preliminary mechanical model of the two-story shear building system is developed by using a lumped parameter approach. Subsequently, a more realistic second-order model of the frame structure is obtained directly from input-output experimental data. To this end, a numerical procedure based on the combination of the Observer/Kalman Filter Identification Method (OKID) with the Eigensystem Realization Algorithm (ERA) is employed for determining the sequence of system Markov parameters. In particular, the fundamental matrices that characterize the state-space representation of a general linear time-invariant dynamical system are obtained from the identified system Markov parameters. In addition to the identified first-order state space model, a second-order mechanical model of the frame structure is experimentally obtained employing a methodology for constructing mechanical models from identified state-space representations. More importantly, considering the assumption of proportional damping, an effective method based on a simple least-square approach is used for calculating an improved estimation of the identified damping coefficients. The experimental modal parameters found by using the proposed methodology are consistent with those predicted by using the analytical approach based on the simplified lumped parameter model. Furthermore, the mechanical model identified employing the approach discussed in this paper is used for developing an actively controlled inertial-based vibration absorber based on the Linear Quadratic Gaussian (LQG) control and estimation method. The numerical and experimental results found in this investigation confirmed the effectiveness of the methodology developed in the paper.

Index Terms—Applied system identification, Experimental modal analysis, Two-story shear building system, Observer/Kalman Filter Identification Method (OKID), Eigensystem Realization Algorithm (ERA), Damping estimation, Linear Quadratic Gaussian (LQG) control and estimation.

I. INTRODUCTION

In many problems of physics and engineering, the development of a mathematical model of a mechanical system is based on a priori theoretical knowledge of the physical behavior of the system of interest. Applied system identification, on the other hand, is concerned with the process of developing mathematical models of physical systems based only on input-output experimental measurements [1], [2], [3], [4], [5], [6], [7]. In engineering applications, a dynamical

model of a mechanical system identified from experimental data can be used for performing the system modal analysis, to predict the system response to known external actions, and in the design process of control strategies necessary for obtaining a desired dynamic behavior [8], [9], [10], [11], [12]. In all these cases, having an accurate mathematical model of a physical system is of fundamental importance for performing numerical experiments based on dynamic simulations [13], [14], [15], [16]. In particular, understanding the dynamic behavior of the mechanical system of interest is of paramount importance in the design process of robust and effective control actions [17], [18], [19]. Also, the parameter identification of substantial structural parameters of a mechanical system, such as for example the system mass, stiffness, and damping matrices, is necessary for the experimental estimation of the system capacity of carrying static loads and for assessing the system dynamic response to time-varying external excitations [20]. In order to achieve these goals, several numerical techniques of applied system identification emerged in the fields of dynamic and control engineering [21]. For instance, a large variety of system identification numerical techniques can be used for obtaining from experimental data realistic first-order state-space models of linear mechanical systems that are necessary for the design of feedforward (open-loop) and feedback (closed-loop) control actions [22], [23], [24], [25], [26], [27], [28], [29]. In the literature, several studies focused on developing numerical procedures for identifying linear time-invariant dynamical models of mechanical systems useful for the design of effective control strategies for machines and structures are available [30], [31], [32], [33], [34], [35], [36], [37]. Among the others, important engineering applications of the numerical techniques devised in the field of applied system identification are the identification of multibody models of the suspension mechanisms necessary for implementing active and passive control schemes, the modal parameters identification of civil structures based on mechanical excitations arising from the external environment, and the dynamic testing of mechanical models of aerospace systems useful for refining the numerical solutions obtained from the finite element analysis [38], [39], [40], [41], [42], [43], [44], [45]. From a general perspective, although they are based on a common set of fundamental principles and make use of similar mathematical methods, the numerical techniques employed in the field of applied system identification can be divided into two broad categories: a) frequency-domain system identification methods and b) time-domain system identification methods [46], [47]. Frequency-domain system identification methods address the problem of identifying mathematical models for accurately describing the frequency response of physical systems considering a set of input-output experimental data represented in the frequency domain. The system identifi-

C. M. Pappalardo is with the *Department of Industrial Engineering, University of Salerno*, Via Giovanni Paolo II, 132, 84084 Fisciano, Salerno, ITALY (corresponding author, email: cpappalardo@unisa.it).

D. Guida is with the *Department of Industrial Engineering, University of Salerno*, Via Giovanni Paolo II, 132, 84084 Fisciano, Salerno, ITALY (email: guida@unisa.it).

cation methods based on the frequency domain represent well-known and reliable techniques that can be successfully used for performing the experimental modal analysis of structural systems. This investigation, on the other hand, is focused on the development of a system identification numerical method based on time-domain input and output measurements. In general, the numerical techniques capable of identifying the dynamical models of mechanical systems by using time-domain input-output data can be readily used for developing effective control strategies and accurate state estimation methods based on the methodologies of modern control and optimal estimation theories. As discussed in the paper, this problem is particularly interesting in the case of the development of second-order physical models of mechanical systems in the configuration space starting from first-order state-space representations. The mechanical models identified using time-domain techniques are useful for performing the experimental modal analysis and for solving the vibration control problem of structural systems [48], [49].

This paper is focused on the development of a methodology for identifying first-order and second-order dynamic models of mechanical systems using time-domain input-output experimental data. The goal is to perform the experimental modal analysis of structural systems in order to obtain an accurate dynamic model that can be used for the design of an optimal feedback controller. The proposed method is based on the numerical techniques of applied system identification and is verified experimentally by using a test rig for analyzing the structural vibrations of mechanical systems. The mechanical system considered as the case study for testing the proposed methodology is a frame structure that can be modeled as a two-story shear building system. The two-story shear building system is excited impulsively by using an impact hammer equipped with a load cell capable of recording the input force impressed to the frame structure. The floors of the frame structure are instrumented with piezoelectric transducers that sense the system accelerations in response to the impulsive excitations. By doing so, the output data obtained from the accelerometers placed on the frame structure are monitored and recorded in real time by means of a frequency spectrum analyzer. In order to facilitate the experimental identification process, a preliminary mechanical model of the two-story shear building system is developed by using the analytical methods of classical mechanics and employing a lumped parameter approach. Subsequently, a system identification numerical procedure based on the combination of the Observer/Kalman Filter Identification Method (OKID) with the Eigensystem Realization Algorithm (ERA) is developed for obtaining a first-order state-space model of the frame structure [50], [51], [52], [53]. In addition to the state-space identification method, a methodology for constructing mechanical models from identified state-space representations is derived in the paper for obtaining experimentally a second-order mechanical model of the two-story shear building system [54], [55], [56], [57]. Furthermore, a simple least-square numerical procedure is devised in this work in order to improve the estimation of the damping parameters of the frame structure considering the proportional damping hypothesis. The identified modal parameters of the frame structure obtained by using the

proposed methodology are consistent with those predicted by using the preliminary simple mechanical model based on the lumped parameter approach. Furthermore, the effectiveness of the method developed in this work is verified experimentally by means of simple vibration tests. The methodology proposed in this paper is also used for the optimal design of a control strategy for suppressing the structural vibrations of the mechanical system of interest for this investigation. To this end, the mechanical model identified using the proposed approach is employed for developing an actively controlled inertial-based vibration absorber based on the Linear Quadratic Gaussian (LQG) control and estimation approach. The actively controlled inertial-based vibration absorber is realized using a physical pendulum hinged on the second floor of the frame structure. The pendulum system is controlled using a brushless motor and the feedback control action is computed in real time by using a digital controller. Numerical and experimental results show that the action of the feedback controller designed using the proposed control architecture leads to a considerable reduction of the vibrations of the two-story shear building system.

This paper is organized as follows. In section 2, a concise description of the mechanical system considered in this investigation as the case study and an illustration of the test rig used for the experimental testing of the proposed identification procedure are provided. In section 3, a simplified lumped parameter model of the frame structure is developed. In section 4, the computational steps of the system identification numerical procedure used in this investigation are described. In section 5, the proposed system identification numerical procedure based on the sequence of system Markov parameters obtained from experimental input-output data is used for determining first-order and second-order mathematical models of the two-story frame structure. In section 6, the development and the implementation of a feedback control system for reducing the structural vibrations of the two-story shear building system considered in this work are described. In section 7, the conclusions drawn in this study and practical considerations for future investigations are discussed.

II. TEST RIG DESCRIPTION

In this section, a concise description of the mechanical system considered as case study and an illustration of the test rig used for the experimental testing of the proposed identification procedure are provided. The mechanical system of interest for the experimental modal analysis carried out in this investigation is the frame structure shown in figure 1. The frame structure examined in this paper can be modeled as a two-story shear building system. In particular, the two-story shear building system is formed by four flexible beams and two rigid connecting rods. The connecting rods are made of aluminum and the flexible beams are made of harmonic steel. The frequency range of interest for testing the dynamic behavior of the frame structure includes all the excitation frequencies between 0 Hz and 15 Hz. In the frequency range of interest, the connecting rods can be considered as rigid bodies while the flexible beams can be assumed as linear elastic continuum bodies. Thus, the frame structure can be modeled as a two-story shear building system deployed in a plane. The current configuration of the two-story shear building system is devised in a way such that an actively



Fig. 1. Frame structure

controlled inertial-based vibration absorber can be placed on the second floor of the frame structure in order to test new control strategies for suppressing the structural vibrations. The experimental apparatus used in this investigation is shown in figure 2. The two floors of the frame structure

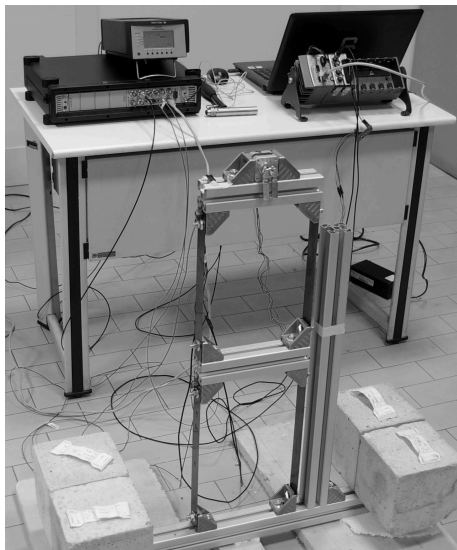


Fig. 2. Test rig

are excited employing an impact hammer instrumented with a load cell that is connected to a spectrum analyzer used for acquiring the experimental data necessary for performing the experimental modal analysis. By doing so, the impulsive forces impressed to the frame structure can be acquired and used as input signals. Piezoelectric transducers for measuring the acceleration of the mechanical system are located on the two floors of the frame structure in order to obtain the time response of the two-story shear building system corresponding to the impulsive excitations. For this purpose, the acceleration signals obtained employing the piezoelectric

transducers are recorded by using the spectrum analyzer in order to obtain the input-output experimental data necessary for applying the system identification numerical procedure developed in this work.

III. MECHANICAL MODEL

In this section, a simplified lumped parameter model of the frame structure is developed. The lumped parameter model developed in this section describes the vibratory behavior of the two-story shear building system in a simplified but realistic manner. The preliminary modal analysis of the frame structure based on the simplified lumped parameter model developed in this section will facilitate the experimental modal analysis based on the proposed identification method. Figure 3 shows a schematic representation of the lumped parameter model used for the preliminary modal analysis of the frame structure. In the lumped parameter model of the

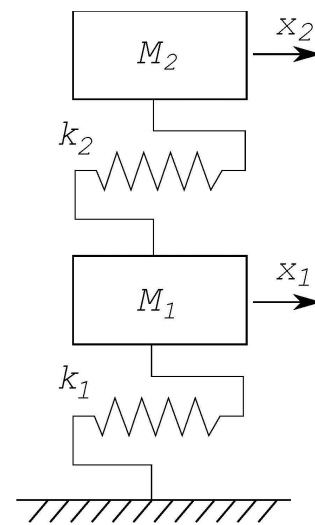


Fig. 3. Lumped parameter model

frame structure, it is assumed that the connecting rods can be modeled as two lumped masses whereas the flexible beams are schematized as two spring elements. Thus, the lumped parameter model of the two-story shear building system has $n_2 = 2$ degrees of freedom. The degrees of freedom of the two-story shear building system are the horizontal displacement of the first and second floors denoted, respectively, as $x_1(t)$ and $x_2(t)$, where t is time. The configuration vector of the two-story shear building system is denoted with $\mathbf{x}(t)$ and is given by:

$$\mathbf{x}(t) = [x_1(t) \quad x_2(t)]^T \quad (1)$$

The equations of motion that mathematically describe the mechanical model of the two-story shear building system can be written in a compact matrix form as:

$$\mathbf{M} \ddot{\mathbf{x}}(t) + \mathbf{K} \mathbf{x}(t) = \mathbf{0} \quad (2)$$

where $\ddot{\mathbf{x}}(t)$ represents the system generalized acceleration vector, $\mathbf{x}(t)$ is the system generalized coordinate vector, \mathbf{M} denotes the system mass matrix, and \mathbf{K} identifies the system stiffness matrix. In the equations of motion, the damping of the mechanical system is neglected because a realistic estimation of the structural damping based only on theoretical

considerations is difficult to obtain. However, a simple and effective method is used in the paper for obtaining a realistic estimation of the system structural damping employing the identified modal parameters obtained from real input-output data. On the other hand, by using the classical methods of analytical dynamics, the mass and stiffness matrices of the lumped parameter model can be written as follows:

$$\mathbf{M} = \text{diag}(m_{1,1}, m_{2,2}) \quad (3)$$

$$\mathbf{K} = \begin{bmatrix} k_{1,1} & k_{1,2} \\ k_{2,1} & k_{2,2} \end{bmatrix} \quad (4)$$

The mass and stiffness matrices \mathbf{M} and \mathbf{K} of the two-story shear building system are constant symmetric positive-definite matrices. For the two-story shear building model, the entries $m_{i,j}$ and $k_{i,j}$ of the system mass and stiffness matrices are defined as:

$$\begin{cases} m_{1,1} = m_1 \\ m_{2,2} = m_2 \end{cases} \quad (5)$$

$$\begin{cases} k_{1,1} = 2k \\ k_{1,2} = k_{2,1} = -k \\ k_{2,2} = k \end{cases} \quad (6)$$

In particular, assuming clamped-clamped boundary conditions and a parallel configuration of the resulting lumped spring elements, the stiffness of each flexible beam can be readily computed as follows:

$$k = 24EJ/L^3 \quad (7)$$

where $m_1 = 0.65$ (kg) and $m_2 = 1.55$ (kg) are respectively the masses of the first and second connecting rods, $E = 2.0 \cdot 10^{11}$ (N/m²) identifies the Young modulus of the flexible beams, $J = 2.917 \cdot 10^{-12}$ (m⁴) is the second moment of area of the flexible beams, and $L = 300 \cdot 10^{-3}$ (m) represents the length of the flexible beams. From a modal analysis of the lumped parameter model of the two-story building system, one obtains the system natural frequencies $f_{n,j}$ and the system modal shapes φ_j . In particular, the normal mode vectors can be analytically expressed as follows:

$$\varphi_j = e^{i\Theta_j} \rho_j, \quad j = 1, 2, \dots, n_2 \quad (8)$$

where e is the Napier's constant, $i = \sqrt{-1}$ is the imaginary unit, ρ_j represents the vector of relative amplitudes corresponding to the mode j , and Θ_j denotes a diagonal matrix containing the relative phases associated with each component of the mode j . Considering the mechanical model of the frame structure, the modal analysis yields the following set of modal parameters:

$$\begin{cases} f_{n,1} = 1.949 \text{ (Hz)} \\ \rho_1 = [1 \quad 1.812]^T \\ \Theta_1 = \text{diag}(0, 0) \end{cases} \quad (9)$$

$$\begin{cases} f_{n,2} = 6.715 \text{ (Hz)} \\ \rho_2 = [1 \quad 0.231]^T \\ \Theta_2 = \text{diag}(0, 3.141) \end{cases} \quad (10)$$

As expected, the first mode shape of the simplified lumped parameter model of the frame structure is perfectly in phase has no nodes, while the second mode has one node and is perfectly out of phase. Although the lumped parameter model represents a crude approximation of the vibratory behavior

of the two-story shear building system, the modal parameters obtained from the preliminary modal analysis performed for the simplified mechanical model of the frame structure are useful for corroborating the numerical results obtained by using the system identification method developed in this investigation.

IV. SYSTEM IDENTIFICATION NUMERICAL PROCEDURE

In this section, the computational steps of the system identification numerical procedure used in this investigation are described. For this purpose, the definition of the Markov parameters is used for identifying the time-domain input-output relationship representing the dynamic properties of a general linear mechanical system. Consider the discrete-time representation of the state-space model of a general linear mechanical system defined by using the following dynamic and measurement equations:

$$\begin{cases} \mathbf{z}(k+1) = \mathbf{A}\mathbf{z}(k) + \mathbf{B}\mathbf{u}(k) \\ \mathbf{y}(k) = \mathbf{C}\mathbf{z}(k) + \mathbf{D}\mathbf{u}(k) \end{cases} \quad (11)$$

where k is the discrete time, $\mathbf{z}(k)$ denotes the discrete-time state vector of dimension $n = 2n_2$, $\mathbf{u}(k)$ identifies the discrete-time input vector of dimension r , $\mathbf{y}(k)$ indicates the discrete-time output vector of dimension m , \mathbf{A} is the discrete-time system state matrix of dimension $n \times n$, \mathbf{B} denotes the discrete-time input influence matrix of dimension $n \times r$, \mathbf{C} identifies the output influence matrix of dimension $m \times n$, and \mathbf{D} indicates the direct transmission matrix of dimension $m \times r$. The discrete-time state-space model can be modified by using a state observer in order to provide an estimation of system state based on inputs and outputs measurements. Thus, the set of discrete-time dynamic and measurement equations can be reformulated considering the introduction of a state estimator as follows:

$$\begin{cases} \hat{\mathbf{z}}(k+1) = \bar{\mathbf{A}}\hat{\mathbf{z}}(k) + \bar{\mathbf{B}}\mathbf{v}(k) \\ \hat{\mathbf{y}}(k) = \mathbf{C}\hat{\mathbf{z}}(k) + \mathbf{D}\mathbf{u}(k) \end{cases} \quad (12)$$

where $\hat{\mathbf{z}}(k)$ denotes the estimated state vector of dimension n , $\hat{\mathbf{y}}(k)$ identifies the estimated measurement vector of dimension m , $\bar{\mathbf{A}}$ is the discrete-time observer state matrix of dimension $n \times n$, $\bar{\mathbf{B}}$ indicates the discrete-time observer state influence matrix of dimension $n \times (r+m)$, and $\mathbf{v}(k)$ represents the generalized input vector of dimension $r+m$ which are respectively defined as:

$$\bar{\mathbf{A}} = \mathbf{A} + \mathbf{G}\mathbf{C} \quad (13)$$

$$\bar{\mathbf{B}} = [\mathbf{B} + \mathbf{G}\mathbf{D} \quad -\mathbf{G}] \quad (14)$$

$$\mathbf{v}(k) = \begin{bmatrix} \mathbf{u}(k) \\ \mathbf{y}(k) \end{bmatrix} \quad (15)$$

where \mathbf{G} is the observer matrix of dimension $n \times m$. The introduction of the observer matrix \mathbf{G} modifies the eigenvalues of the observer state matrix $\bar{\mathbf{A}}$ which can be made as asymptotically stable as desired. Thus, the discrete-time state-space model and the discrete-time observer state-space model lead to linear input-output relationships associated with the dynamic behavior of a general linear time-invariant

mechanical system which can be respectively expressed as follows:

$$\mathbf{y}(k) = \sum_{j=0}^k (\mathbf{Y}_j \mathbf{u}(k-j)) \quad (16)$$

$$\hat{\mathbf{y}}(k) = \sum_{j=0}^k (\bar{\mathbf{Y}}_j \mathbf{v}(k-j)) \quad (17)$$

where \mathbf{Y}_k is a sequence of $m \times r$ matrices called system Markov parameters, whereas $\bar{\mathbf{Y}}_k$ is a sequence of $m \times (r+m)$ matrices known as observer Markov parameters. The system Markov parameters and the observer Markov parameters are also referred to as discrete impulse response functions because they represent the response of the discrete-time system and observer state-space models to impulsive excitations. The system and observer Markov parameters denoted with the matrices \mathbf{Y}_k and $\bar{\mathbf{Y}}_k$ are respectively defined as follows:

$$\begin{cases} \mathbf{Y}_0 = \mathbf{D} \\ \mathbf{Y}_k = \mathbf{C}\mathbf{A}^{k-1}\mathbf{B} \end{cases} \quad (18)$$

$$\begin{cases} \bar{\mathbf{Y}}_0 = \mathbf{D} \\ \bar{\mathbf{Y}}_k = \mathbf{C}\bar{\mathbf{A}}^{k-1}\bar{\mathbf{B}} \end{cases} \quad (19)$$

In the computer implementation of system identification algorithms based on a set of time-domain input-output data, an additional sequence of Markov parameters known as observer gain Markov parameters can be defined. The sequence of observer gain Markov parameters is useful for developing system identification numerical procedures and is given by:

$$\begin{cases} \mathbf{Y}_0^0 = \mathbf{D} \\ \mathbf{Y}_k^0 = \mathbf{C}\mathbf{A}^{k-1}\mathbf{G} \end{cases} \quad (20)$$

where the sequence of rectangular matrices \mathbf{Y}_k^0 of dimension $m \times m$ denotes the observer gain Markov parameters. The set of observer Markov parameters $\bar{\mathbf{Y}}_k$ can be computed from measured input-output data employing a computational procedure based on a least-square approximation method. On the other hand, once that the observer Markov parameters $\bar{\mathbf{Y}}_k$ are identified starting from experimental data, a recursive procedure can be used to recover the sequence of system Markov parameters \mathbf{Y}_k and the sequence of observer gain Markov parameters \mathbf{Y}_k^0 from the identified set of observer Markov parameters $\bar{\mathbf{Y}}_k$. In order to achieve this goal, consider a finite difference input-output representation of a linear mechanical system described by using the following equations:

$$\mathbf{y}(k) + \sum_{j=1}^p \left(\bar{\mathbf{Y}}_j^{(2)} \mathbf{y}(k-j) \right) = \quad (21)$$

$$\sum_{j=1}^p \left(\bar{\mathbf{Y}}_j^{(1)} \mathbf{u}(k-j) \right) + \mathbf{D}\mathbf{u}(k)$$

where $\bar{\mathbf{Y}}_k^{(1)}$ and $\bar{\mathbf{Y}}_k^{(2)}$ are rectangular matrices of dimensions $m \times r$ and $m \times m$ that are respectively defined as:

$$\begin{cases} \bar{\mathbf{Y}}_k^{(1)} = \mathbf{C}(\mathbf{A} + \mathbf{G}\mathbf{C})^{k-1}(\mathbf{B} + \mathbf{G}\mathbf{D}) \\ \bar{\mathbf{Y}}_k^{(2)} = \mathbf{C}(\mathbf{A} + \mathbf{G}\mathbf{C})^{k-1}\mathbf{G} \end{cases} \quad (22)$$

The matrix representation of the observer Markov parameters $\bar{\mathbf{Y}}_k$ can be partitioned as follows:

$$\bar{\mathbf{Y}}_k = \begin{bmatrix} \bar{\mathbf{Y}}_k^{(1)} & -\bar{\mathbf{Y}}_k^{(2)} \end{bmatrix} \quad (23)$$

A least-square computational approach based on input-output experimental data can be effectively used for computing the coefficients of the finite difference model. For this purpose, a numerical procedure based on the Observer/Kalman Filter Identification Method (OKID) can be readily used. By doing so, the sequence of observer Markov parameters can be identified and, subsequently, the system Markov parameters and the observer gain Markov parameters can be obtained from experimental measurements. To this end, the linear difference model can be reformulated in a matrix form considering a data record of length l as follows:

$$\mathbf{Y} = \bar{\mathbf{L}}_p \mathbf{V}_p \quad (24)$$

where \mathbf{Y} , $\bar{\mathbf{L}}_p$, and \mathbf{V}_p are rectangular matrices having dimensions $m \times l$, $m \times (r + (r+m)p)$, and $(r + (r+m)p) \times l$ and are respectively defined as follows:

$$\mathbf{Y} = \begin{bmatrix} \mathbf{y}(0) & \mathbf{y}(1) & \dots & \mathbf{y}(l-1) \end{bmatrix} \quad (25)$$

$$\bar{\mathbf{L}}_p = \begin{bmatrix} \bar{\mathbf{Y}}_0 & \bar{\mathbf{Y}}_1 & \dots & \bar{\mathbf{Y}}_p \end{bmatrix} \quad (26)$$

$$\mathbf{V}_p = \begin{bmatrix} \mathbf{u}(0) & \mathbf{u}(1) & \dots & \mathbf{u}(l-1) \\ \mathbf{0} & \mathbf{v}(0) & \dots & \mathbf{v}(l-2) \\ \vdots & \vdots & \ddots & \vdots \\ \mathbf{0} & \mathbf{0} & \dots & \mathbf{v}(l-p-1) \end{bmatrix} \quad (27)$$

where the integer p represents the discrete time at which the approximation of the estimated output vector $\hat{\mathbf{y}}(k)$ approaches the actual measured output vector $\mathbf{y}(k)$. The sequence of the first p observer Markov parameters $\bar{\mathbf{Y}}_k$ is included in the block matrix $\bar{\mathbf{L}}_p$ and, therefore, a simple least-square computational method can be used for obtaining an approximate solution of the observer Markov parameters $\bar{\mathbf{Y}}_k$. Thus, one can write the following set of equations based on experimental input-output measurements:

$$\bar{\mathbf{L}}_p = \mathbf{Y}\mathbf{V}_p^+ \quad (28)$$

where \mathbf{V}_p^+ represents the Moore-Penrose pseudoinverse matrix of the matrix \mathbf{V}_p identified by a rectangular matrix having dimension $m \times (r + (r+m)p)$. Furthermore, the sequence of system Markov parameters \mathbf{Y}_k and the sequence of observer gain Markov parameters \mathbf{Y}_k^0 can be obtained from the identified observer Markov parameters with the use of recursive relationships mathematically defined as:

$$\begin{cases} \mathbf{D} = \mathbf{Y}_0 = \bar{\mathbf{Y}}_0 \\ \mathbf{Y}_k = \bar{\mathbf{Y}}_k^{(1)} - \sum_{j=1}^k \bar{\mathbf{Y}}_j^{(2)} \mathbf{Y}_{k-j}, \quad k = 1, 2, \dots, p \\ \mathbf{Y}_k = - \sum_{j=1}^p \bar{\mathbf{Y}}_j^{(2)} \mathbf{Y}_{k-j}, \quad k = p+1, p+2, \dots \end{cases} \quad (29)$$

$$\left\{ \begin{array}{l} \mathbf{Y}_1^0 = \mathbf{C}\mathbf{G} = \bar{\mathbf{Y}}_1^{(2)} \\ \mathbf{Y}_k^0 = \bar{\mathbf{Y}}_k^{(2)} - \sum_{j=1}^{k-1} \bar{\mathbf{Y}}_j^{(2)} \mathbf{Y}_{k-j}^0, \quad k = 2, 3, \dots, p \\ \mathbf{Y}_k^0 = - \sum_{j=1}^p \bar{\mathbf{Y}}_j^{(2)} \mathbf{Y}_{k-j}^0, \quad k = p+1, p+2, \dots \end{array} \right. \quad (30)$$

An applied system identification methodology based on time domain data can be developed by using the combination of the identified system and observer gain Markov parameters \mathbf{Y}_k and \mathbf{Y}_k^0 . To this end, the Eigensystem Realization Algorithm (ERA) is a computational procedure based on the identified Markov parameters which can be readily used for computing a set of state-space matrices \mathbf{A} , \mathbf{B} , \mathbf{C} , and \mathbf{D} of a general linear mechanical system. Thus, consider the following block matrix that includes the system and observer gain Markov parameters:

$$\mathbf{\Gamma}_k = \begin{bmatrix} \mathbf{Y}_k & \mathbf{Y}_k^0 \end{bmatrix} \quad (31)$$

where $\mathbf{\Gamma}_k$ is a block matrix of dimensions $m \times (r+m)$. The assembly of the combined matrix $\mathbf{\Gamma}_k$ is used for constructing a generalized block Hankel matrix defined as follows:

$$\bar{\mathbf{N}}(k-1) = \begin{bmatrix} \mathbf{\Gamma}_k & \mathbf{\Gamma}_{k+1} & \dots & \mathbf{\Gamma}_{k+\beta-1} \\ \mathbf{\Gamma}_{k+1} & \mathbf{\Gamma}_{k+2} & \dots & \mathbf{\Gamma}_{k+\beta} \\ \vdots & \vdots & \ddots & \vdots \\ \mathbf{\Gamma}_{k+\alpha-1} & \mathbf{\Gamma}_{k+\alpha} & \dots & \mathbf{\Gamma}_{k+\alpha+\beta-2} \end{bmatrix} \quad (32)$$

where $\bar{\mathbf{N}}(k-1)$ is a block Hankel matrix of dimensions $\alpha m \times \beta(r+m)$ in which the set of system and observer gain Markov parameters \mathbf{Y}_k and \mathbf{Y}_k^0 are included. In the block Hankel matrix $\bar{\mathbf{N}}(k-1)$, the two integers α and β are numerical parameters which can be assumed as $\alpha = p$ and $\beta = l - p$, where l is the length of the data record. In particular, the generalized Hankel matrix $\bar{\mathbf{N}}(0)$ can be readily factorized using the Singular Value Decomposition (SVD) as follows:

$$\bar{\mathbf{N}}(0) = \bar{\mathbf{R}}\bar{\mathbf{\Sigma}}\bar{\mathbf{S}}^T \quad (33)$$

where the rectangular matrix $\bar{\mathbf{\Sigma}}$ contains the singular values of the generalized Hankel matrix $\bar{\mathbf{N}}(0)$ and the columns of the matrices $\bar{\mathbf{R}}$ and $\bar{\mathbf{S}}$ form orthonormal vectors. The block matrix $\bar{\mathbf{\Sigma}}$ can be partitioned as follows:

$$\bar{\mathbf{\Sigma}} = \begin{bmatrix} \bar{\mathbf{\Sigma}}_{\hat{n}} & \mathbf{O} \\ \mathbf{O} & \mathbf{O} \end{bmatrix} \quad (34)$$

where the submatrix $\bar{\mathbf{\Sigma}}_{\hat{n}}$ is a square diagonal matrix defined as:

$$\bar{\mathbf{\Sigma}}_{\hat{n}} = \text{diag}(\sigma_1, \sigma_2, \dots, \sigma_{\hat{n}}) \quad (35)$$

where $\sigma_i, i = 1, 2, \dots, \hat{n}$ represent the nonzero singular values associated with the generalized Hankel matrix $\bar{\mathbf{N}}(0)$. Moreover, the generalized Hankel matrix $\bar{\mathbf{N}}(0)$ and its Moore-Penrose pseudoinverse matrix $\bar{\mathbf{N}}^+(0)$ can be respectively written as follows:

$$\bar{\mathbf{N}}(0) = \bar{\mathbf{R}}_{\hat{n}}\bar{\mathbf{\Sigma}}_{\hat{n}}\bar{\mathbf{S}}_{\hat{n}}^T \quad (36)$$

$$\bar{\mathbf{N}}^+(0) = \bar{\mathbf{S}}_{\hat{n}}\bar{\mathbf{\Sigma}}_{\hat{n}}^{-1}\bar{\mathbf{R}}_{\hat{n}}^T \quad (37)$$

where $\bar{\mathbf{R}}_{\hat{n}}$ and $\bar{\mathbf{S}}_{\hat{n}}$ represent the rectangular matrices formed by the first \hat{n} columns of the rectangular matrices $\bar{\mathbf{R}}$ and

$\bar{\mathbf{S}}$. A thorough analysis of the spectrum of the singular values $\sigma_i, i = 1, 2, \dots, \hat{n}$ of the generalized Hankel matrix $\bar{\mathbf{N}}(0)$ allows for establishing the order \hat{n} of the identified state-space model of the linear mechanical system under consideration. By doing so, an identified discrete-time state-space model can be computed leading to the discrete-time state-space matrices $\hat{\mathbf{A}}$, $\hat{\mathbf{B}}$, $\hat{\mathbf{C}}$, and $\hat{\mathbf{D}}$ as well as to the identified observer matrix $\hat{\mathbf{G}}$. The set of discrete-time state-space matrices obtained from the sequence of system Markov parameters based on the measured of input-output data can be readily obtained as follows:

$$\left\{ \begin{array}{l} \hat{\mathbf{A}} = \bar{\mathbf{\Sigma}}_{\hat{n}}^{-1/2} \bar{\mathbf{R}}_{\hat{n}}^T \bar{\mathbf{N}}(1) \bar{\mathbf{S}}_{\hat{n}} \bar{\mathbf{\Sigma}}_{\hat{n}}^{-1/2} \\ [\hat{\mathbf{B}} \quad \hat{\mathbf{G}}] = \bar{\mathbf{\Sigma}}_{\hat{n}}^{-1/2} \bar{\mathbf{S}}_{\hat{n}}^T \mathbf{E}_{r+m} \\ \hat{\mathbf{C}} = \mathbf{E}_m^T \bar{\mathbf{R}}_{\hat{n}} \bar{\mathbf{\Sigma}}_{\hat{n}}^{-1/2} \\ \hat{\mathbf{D}} = \mathbf{Y}_0 = \bar{\mathbf{Y}}_0 \end{array} \right. \quad (38)$$

where \mathbf{E}_m and \mathbf{E}_{r+m} are Boolean matrices given by:

$$\mathbf{E}_m^T = [\mathbf{I}_m \quad \mathbf{O}_m \quad \dots \quad \mathbf{O}_m]^T \quad (39)$$

$$\mathbf{E}_{r+m}^T = [\mathbf{I}_{r+m} \quad \mathbf{O}_{r+m} \quad \dots \quad \mathbf{O}_{r+m}]^T \quad (40)$$

The set of identified discrete-time state-space matrices $\hat{\mathbf{A}}$, $\hat{\mathbf{B}}$, $\hat{\mathbf{C}}$, $\hat{\mathbf{D}}$, and $\hat{\mathbf{G}}$ represents a minimum order, controllable, and observable state-space realization of a general mechanical system having a linear mathematical structure. The modal parameters of the identified mechanical model represent the actual system modal parameters obtained by the available sequence of input-output data. In particular, the discrete-time state-space model of the mechanical system can be readily transformed into its continuous-time counterpart. More importantly, a second-order mechanical model of the dynamical system can be obtained by using the identified modal parameters of the state-space model as follows:

$$\left\{ \begin{array}{l} \hat{\mathbf{M}} = (\hat{\mathbf{W}}\hat{\mathbf{\Lambda}}_c\hat{\mathbf{W}}^T)^{-1} \\ \hat{\mathbf{K}} = -(\hat{\mathbf{W}}\hat{\mathbf{\Lambda}}_c^{-1}\hat{\mathbf{W}}^T)^{-1} \\ \hat{\mathbf{R}} = -(\hat{\mathbf{M}}\hat{\mathbf{W}}\hat{\mathbf{\Lambda}}_c^2\hat{\mathbf{W}}^T\hat{\mathbf{M}}) \end{array} \right. \quad (41)$$

where $\hat{\mathbf{\Lambda}}_c$ is the diagonal matrix containing the identified eigenvalues of the continuous-time state-space model, $\hat{\mathbf{W}}$ indicates the matrix of the identified eigenvectors associated with the set of system generalized coordinates, $\hat{\mathbf{M}}$ represents the identified mass matrix, $\hat{\mathbf{K}}$ is the identified stiffness matrix, and $\hat{\mathbf{R}}$ denotes the identified damping matrix of the linear model of the mechanical system. In practical applications, the estimation of the system damping matrix $\hat{\mathbf{R}}$ is considerably influenced by the noise that affects the input-output data set. Therefore, an improved estimation method of the identified damping matrix $\hat{\mathbf{R}}$ of the mechanical system should be employed for obtaining more realistic numerical results. For this purpose, a simple least-square estimation method based on the proportional damping assumption is employed in this paper for obtaining the proportional damping coefficients $\hat{\alpha}$ and $\hat{\beta}$. The method used in this work for

calculating the proportional damping coefficients $\hat{\alpha}$ and $\hat{\beta}$ can be mathematically written as follows:

$$\bar{\mathbf{x}} = \bar{\mathbf{C}}^+ \bar{\mathbf{d}} \quad (42)$$

where the matrix $\bar{\mathbf{C}}$ and the vectors $\bar{\mathbf{d}}$ and $\bar{\mathbf{x}}$ are respectively defined as:

$$\bar{\mathbf{x}} = \begin{bmatrix} \hat{\alpha} \\ \hat{\beta} \end{bmatrix} \quad (43)$$

$$\bar{\mathbf{C}} = \frac{1}{2} \begin{bmatrix} \frac{1}{2\pi\hat{f}_{n,1}} & 2\pi\hat{f}_{n,1} \\ \frac{1}{2\pi\hat{f}_{n,2}} & 2\pi\hat{f}_{n,2} \\ \vdots & \vdots \\ \frac{1}{2\pi\hat{f}_{n,\hat{n}_2}} & 2\pi\hat{f}_{n,\hat{n}_2} \end{bmatrix} \quad (44)$$

$$\bar{\mathbf{d}} = \begin{bmatrix} \hat{\xi}_1 \\ \hat{\xi}_2 \\ \vdots \\ \hat{\xi}_{\hat{n}_2} \end{bmatrix} \quad (45)$$

where $\bar{\mathbf{C}}^+$ denotes the Moore-Penrose pseudoinverse matrix of the coefficient matrix $\bar{\mathbf{C}}$, $\hat{f}_{n,j}$ represents the identified natural frequency associated with the mode j of the mechanical system, and $\hat{\xi}_j$ is the identified damping ratio relative to the mode j of the linear dynamical system. Subsequently, an improved estimation of the system damping matrix $\hat{\mathbf{R}}$ based on the proportional damping assumption can be readily obtained as follows:

$$\hat{\mathbf{R}} = \hat{\alpha}\hat{\mathbf{M}} + \hat{\beta}\hat{\mathbf{K}} \quad (46)$$

where the proportional damping coefficients $\hat{\alpha}$ and $\hat{\beta}$ are calculated from the identified modal parameters by using the proposed least-square approximation method.

V. EXPERIMENTAL MODAL ANALYSIS

In this section, the proposed system identification numerical procedure based on the sequence of system Markov parameters obtained from experimental input-output data is used for determining a mathematical model of the two-story frame structure. Subsequently, the system modal parameters are obtained by performing an experimental modal analysis. In order to achieve this goal, an impact hammer instrumented with a load cell is used to excite impulsively the first floor of the two-story shear building system and the corresponding accelerations of the two floors of the frame structure are recorded by using piezoelectric transducers. The impulsive force signal obtained by using the load cell of the impact hammer is shown in figure 4. The acceleration signals of the frame structure recorded in correspondence of the impulsive excitation by using the piezoelectric transducers placed on the two floors of the two-story shear building system are respectively shown in figures 5 and 6. The sampling frequency used for obtaining the experimental data is $f_s = 32$ (Hz), whereas the time span considered is $T_s = 32$ (s). The sampling time step is $\Delta t = 3.125 \cdot 10^{-2}$ (s) which corresponds to a Nyquist frequency of $f_N = 16$ (Hz). Therefore, the frequency range of interest spanning from 0 Hz to 15 Hz is correctly captured by the experimental input-output data acquired during the experimental testing. The experimental sequences of input-output data were filtered in the frequency domain. To this end, a low-pass

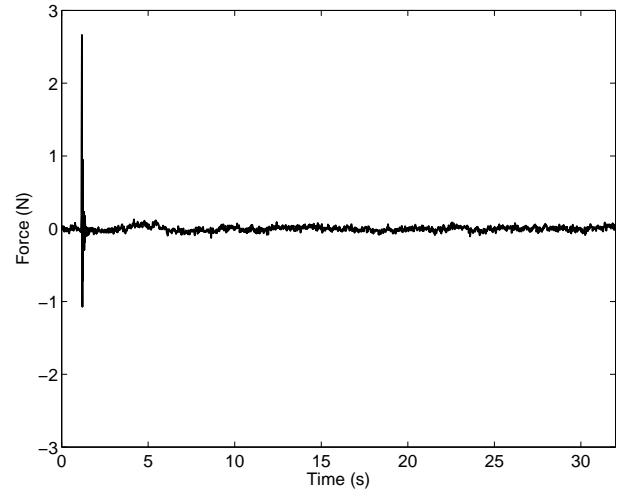


Fig. 4. Force input measurement

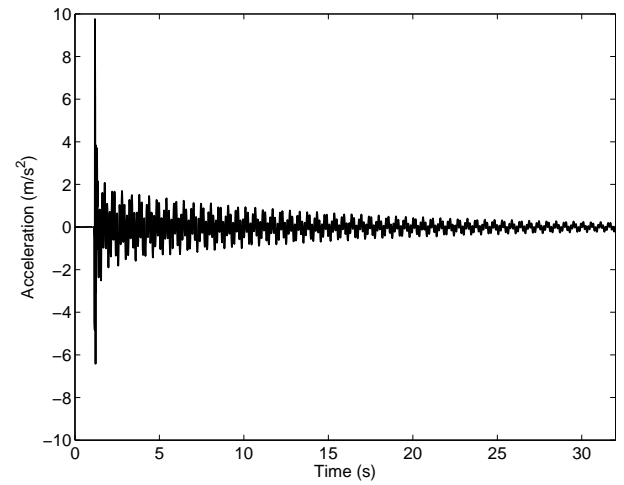


Fig. 5. Acceleration output measurement of the first floor

filter having a cut-off frequency of $f_c = 16$ (Hz) was used for eliminating the influence of high-frequency noise. By using the proposed system identification numerical procedure based on the set of input-output data obtained by means of experimental measurements, the set of observer Markov parameters $\bar{\mathbf{Y}}_k$ was identified. Subsequently, the system Markov parameters \mathbf{Y}_k and the observer gain Markov parameters \mathbf{Y}_k^0 were recovered from the identified sequence of the observer Markov parameters $\bar{\mathbf{Y}}_k$. Then, the matrix sequence of the combined Markov parameters Γ_k was assembled by using the identified Markov parameters $\bar{\mathbf{Y}}_k$ and the identified observer gain Markov parameters \mathbf{Y}_k^0 employing recursive relationships. The combined Markov parameters Γ_k were subsequently used to construct the sequence of Hankel matrices $\bar{\mathbf{N}}(k-1)$ necessary for implementing the proposed system identification method. In this process, the Hankel matrix $\bar{\mathbf{N}}(0)$ was factorized by using the Singular Value Decomposition (SVD) method. Figure 7 shows the magnitude of the singular values of the identified Hankel matrix $\bar{\mathbf{N}}(0)$. As shown in figure 7, only 4 singular values have a relatively large magnitude. Consequently, the order of the identified state-space model representing mathematically the two-story shear building system is $\hat{n} = 4$. Thus, the

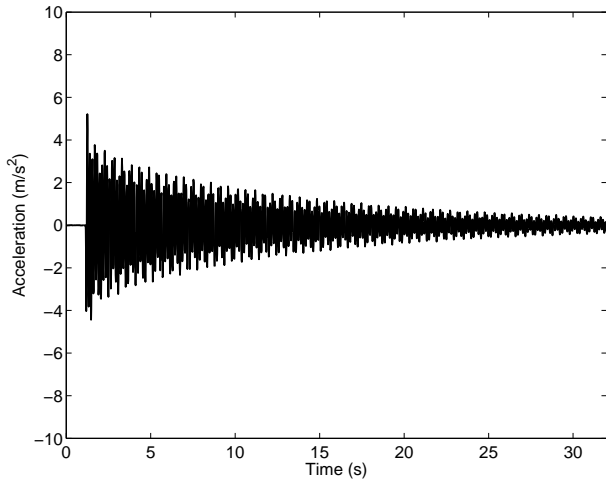


Fig. 6. Acceleration output measurement of the second floor

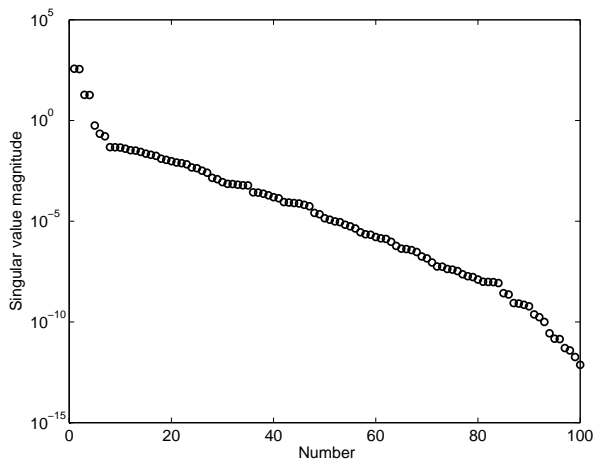


Fig. 7. Magnitude of the singular values of the identified Hankel matrix

identified discrete-time state-space matrices $\hat{\mathbf{A}}$, $\hat{\mathbf{B}}$, $\hat{\mathbf{C}}$, and $\hat{\mathbf{D}}$ corresponding to the identified linear dynamical model of the two-story frame structure and the identified observer matrix $\hat{\mathbf{G}}$ can be computed by using the system identification approach developed in this work leading to the following set of identified modal parameters:

$$\begin{cases} \hat{f}_{n,1} = 1.912 \text{ (Hz)} \\ \hat{\xi}_1 = 0.0118 \\ \hat{\rho}_1 = [1 \quad 0.937]^T \\ \hat{\Theta}_1 = \text{diag}(0, 0.1076) \end{cases} \quad (47)$$

$$\begin{cases} \hat{f}_{n,2} = 6.847 \text{ (Hz)} \\ \hat{\xi}_2 = 0.0039 \\ \hat{\rho}_2 = [1 \quad 2.180]^T \\ \hat{\Theta}_2 = \text{diag}(0, -3.1642) \end{cases} \quad (48)$$

where $\hat{f}_{n,j}$ represents the identified natural frequency of the mode j , $\hat{\xi}_j$ indicates the identified damping ratio corresponding to the mode j , $\hat{\rho}_j = e^{i\hat{\Theta}_j} \hat{\rho}_j$ is the identified modal vector of the mode j , $\hat{\rho}_j$ denotes the identified vector of relative modal amplitudes of the mode j , and $\hat{\Theta}_j$ identifies the relative phase matrix of the mode j . It is important to note that the modal parameters of the identified continuous-time

state-space model are consistent with those obtained by using the approximate modal analysis based on the preliminary lumped parameter model of the frame structure. Furthermore, a preliminary estimation of the system structural damping is obtained from the identified modal parameters. However, since the magnitude of the identified modal damping is small, the identified mode shapes can be assumed approximately in phase or perfectly out of phase. Therefore, the hypothesis of proportional damping can be employed and the proposed method for identifying the proportional damping coefficients can be used for improving the estimation of the damping coefficients. By doing so, the proportional damping coefficients can be readily computed to yield:

$$\begin{cases} \hat{\alpha} = 0.1752 \\ \hat{\beta} = 3.4355 \cdot 10^{-5} \end{cases} \quad (49)$$

where $\hat{\alpha}$ and $\hat{\beta}$ are the identified proportional damping coefficients obtained by using the simple least-square estimation method developed in this investigation. Moreover, a second-order mechanical model can be constructed from the identified state-space representation by using the methodology discussed in the paper leading to the following set of identified matrices:

$$\hat{\mathbf{M}} = \begin{bmatrix} 1.3005 & -0.0846 \\ -0.0846 & 0.5663 \end{bmatrix} \quad (50)$$

$$\hat{\mathbf{K}} = \begin{bmatrix} 1047.3 & -824.1 \\ -824.1 & 841.6 \end{bmatrix} \quad (51)$$

$$\hat{\mathbf{R}} = \begin{bmatrix} 72.8876 & -45.6374 \\ -45.6374 & 46.3942 \end{bmatrix} \quad (52)$$

where $\hat{\mathbf{M}}$ represents the identified mass matrix, $\hat{\mathbf{K}}$ indicates the identified stiffness matrix, and $\hat{\mathbf{R}}$ is the identified damping matrix. An improved estimation of the identified damping matrix $\hat{\mathbf{R}}$ can be obtained employing the proportional damping assumption and considering the identified proportional damping coefficients $\hat{\alpha}$ and $\hat{\beta}$ together with the identified mass and stiffness matrices $\hat{\mathbf{M}}$ and $\hat{\mathbf{K}}$ as follows:

$$\begin{aligned} \hat{\mathbf{R}} &= \hat{\alpha}\hat{\mathbf{M}} + \hat{\beta}\hat{\mathbf{K}} \\ &= \begin{bmatrix} 0.3955 & -0.0485 \\ -0.0485 & 0.1838 \end{bmatrix} \end{aligned} \quad (53)$$

As shown in the next section of the paper, the identified second-order mechanical model of the two-story frame structure can be used for the optimal design of an effective control strategy. The optimal feedback controller is implemented by means of an actively controlled inertial-based vibration absorber and leads to the reduction of the structural vibrations induced by and external source of excitation.

VI. FEEDBACK CONTROL DESIGN

In this section, the development of a feedback controller is described. The feedback controller developed in this section is used for reducing the structural vibration of the two-story building system. The architecture of the feedback controller that is employed for the implementation of the control strategy described in this section is shown in figure 8. As shown in figure 8, the ground of the frame structure is excited by a shaker. The shaker is connected to the

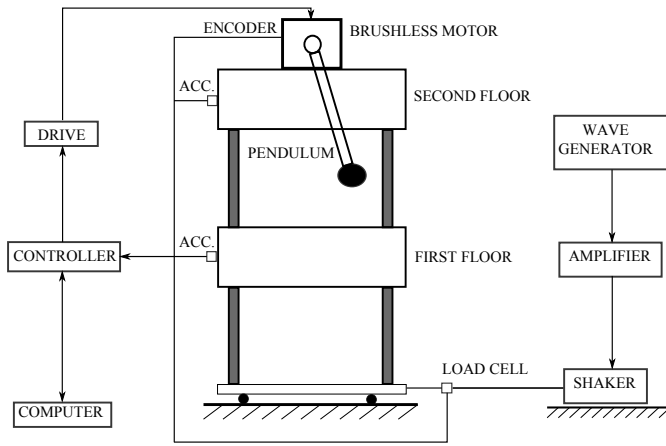


Fig. 8. Control scheme

ground of the two-story structure by means of a stinger. In order to measure the force transferred to the two-story frame structure by the shaker, a load cell is collocated between the ground of the structure and the stinger. The shaker is connected to a power amplifier that receives input signals from an arbitrary wave function generator. In order to measure the mechanical vibrations of the two-story shear building system, piezoelectric transducers that capture the system accelerations are collocated on each floor of the frame structure using the same experimental set-up employed for identifying the dynamic model of the two-story system. Furthermore, a physical pendulum having an additional mass concentrated on the tip is collocated on the second floor of the frame structure. The physical pendulum schematically shown in figure 8 is designed to work as an actively controlled inertial-based vibration absorber. To this end, the physical pendulum is actively controlled using a control actuator driven by a brushless motor. The brushless motor is equipped with an encoder that allows for sensing the pendulum angular rotation. The control actuator provides a control torque that is calculated in real time by using a digital controller. For this purpose, the digital controller communicates with the brushless motor by means of a drive device, reads the acceleration signals obtained from the piezoelectric transducers, and makes use of the force signal measured by the load cell. The digital controller can be programmed offline and monitored online in order to calculate a feedback control law for the control torque of the brushless motor that is based on the force and acceleration measurements. The control method used for the design of the feedback controller is the Linear Quadratic Gaussian (LQG) control approach. This method is implemented by using the identified second-order mechanical model of the two-story frame structure described in the previous section of the paper. More importantly, the optimal design of the feedback controller is performed using the identified second-order mechanical model of the two-story structure in combination with a linear lumped parameter model of an actively controlled inertial-based vibration absorber realized using the actuated pendulum. The updated mechanical model used to design the feedback controller includes $n_2 = 3$ degrees of freedom. The generalized coordinates used in this mechanical model are contained in a configuration vector denoted with

$\mathbf{x}(t)$ and given by $\mathbf{x}(t) = [x_1(t) \ x_2(t) \ \theta(t)]^T$, where $x_1(t)$ and $x_2(t)$ represent the linear displacements of the first and second floors of the frame structure, respectively, while $\theta(t)$ identifies the angular rotation of the pendulum. Employing the mathematical methods of analytical mechanics, the mechanical model of the two-story shear building system with the pendulum hinged on the second floor can be readily obtained as follows:

$$\mathbf{M}\ddot{\mathbf{x}}(t) + \mathbf{R}\dot{\mathbf{x}}(t) + \mathbf{K}\mathbf{x}(t) = \mathbf{T}_e\mathbf{u}_e(t) + \mathbf{T}_c\mathbf{u}_c(t) \quad (54)$$

where $\ddot{\mathbf{x}}(t)$ is the system generalized acceleration vector, $\dot{\mathbf{x}}(t)$ represents the system generalized velocity vector, $\mathbf{x}(t)$ denotes the system generalized coordinate vector, \mathbf{M} is the system mass matrix, \mathbf{R} represents the system damping matrix, \mathbf{K} denotes the system stiffness matrix, $\mathbf{u}_e(t)$ is the vector of uncontrollable inputs, $\mathbf{u}_c(t)$ is the vector of controllable inputs, \mathbf{T}_e is a transformation matrix that identifies the locations of the uncontrollable inputs, and \mathbf{T}_c is a transformation matrix that identifies the locations of the controllable inputs. For the two-story system with the pendulum attached on the second floor, the system mass, stiffness, and damping matrices are respectively defined as follows:

$$\begin{cases} \mathbf{M} = \mathbf{B}_x^T \hat{\mathbf{M}} \mathbf{B}_x + \mathbf{B}_3^T \mathbf{M}_3 \mathbf{B}_3 \\ \mathbf{K} = \mathbf{B}_x^T \hat{\mathbf{K}} \mathbf{B}_x + \mathbf{B}_3^T \mathbf{K}_3 \mathbf{B}_3 \\ \mathbf{R} = \mathbf{B}_x^T \hat{\mathbf{R}} \mathbf{B}_x + \mathbf{B}_3^T \mathbf{R}_3 \mathbf{B}_3 \end{cases} \quad (55)$$

where $\hat{\mathbf{M}}$, $\hat{\mathbf{R}}$, and $\hat{\mathbf{K}}$ denote respectively the identified mass, damping, and stiffness matrices obtained in the previous section of the paper, while \mathbf{M}_3 , \mathbf{R}_3 , and \mathbf{K}_3 represent respectively the mass, damping, and stiffness matrices associated with the physical pendulum that are given by:

$$\mathbf{M}_3 = \begin{bmatrix} m_3 & m_3 l \\ m_3 l & m_3 l^2 + I_{zz,3} \end{bmatrix}, \quad \mathbf{K}_3 = m_3 g l, \quad \mathbf{R}_3 = 0 \quad (56)$$

where $g = 9.81 \text{ (m/s}^2\text{)}$ represents the gravity acceleration, $l = 82.5 \cdot 10^{-3} \text{ (m)}$ is half the length of the pendulum, $m_3 = 0.083 \text{ (kg)}$ denotes the pendulum mass, and $I_{zz,3} = 8.32 \cdot 10^{-4} \text{ (kg} \cdot \text{m}^2\text{)}$ identifies the mass moment of inertia of the pendulum. In these equations, the matrices \mathbf{B}_x and \mathbf{B}_3 are appropriate Boolean matrices that can be used to formulate the complete mechanical model of the two-story frame structure with the pendulum hinged on the second floor. For the two-story shear building system, the vector of uncontrollable inputs $\mathbf{u}_e(t)$ contains an external excitation force applied on the ground of the frame structure, whereas the vector of controllable inputs $\mathbf{u}_c(t)$ includes a control torque applied on the pendulum. Considering a worst-case scenario, the uncontrollable input vector $\mathbf{u}_e(t)$ is equal to an external force $F_e(t)$ defined by the superposition of two harmonic components having large amplitudes and characterized by a set of excitation frequencies close to the first two natural frequencies of the frame structure. Furthermore, in order to simulate the action of the earthquake, the two-story frame structure is excited by a noise excitation source combined with the two harmonic excitations. Therefore, considering the worst case scenario in which the external excitation frequencies are close to the

first two system natural frequencies, the external force $F_e(t)$ modeled as an uncontrollable input is defined as follows:

$$F_e(t) = F_{0,1} \sin(2\pi f_1 t) + F_{0,2} \sin(2\pi f_2 t) + w(t) \quad (57)$$

where $F_{0,1} = 0.1$ (N) and $F_{0,2} = 0.1$ (N) denote the amplitudes of the first and second harmonic forces, respectively, whereas $f_1 = 1.9$ (Hz) and $f_2 = 6.8$ (Hz) represent the frequencies of the first and second harmonic forces, respectively, and $w(t)$ is a noise excitation source characterized by a normal Gaussian distribution. In the identification and control scheme considered in section and showed in figure 8, the external excitation force can be measured using a load cell collocated between the shaker and the stinger, while the measurable output variables of the two-story shear building system are the accelerations of the two floors and the pendulum angular rotation. Consequently, these output variables can be included into an output vector denoted with $\mathbf{y}(t)$ and defined as $\mathbf{y}(t) = [\ddot{x}_1(t) \quad \ddot{x}_2(t) \quad \theta(t)]^T$. The system measurement equations are, therefore, given by:

$$\mathbf{y}(t) = \mathbf{C}_d \mathbf{x}(t) + \mathbf{C}_v \dot{\mathbf{x}}(t) + \mathbf{C}_a \ddot{\mathbf{x}}(t) \quad (58)$$

where \mathbf{C}_d is the generalized displacement influence matrix on the measured output, \mathbf{C}_v is the generalized velocity influence matrix on the measured output, and \mathbf{C}_a is the generalized acceleration influence matrix on the measured output. Considering a time span equal to $T_s = 64$ (s) and a time step equal to $\Delta t = 3.125 \cdot 10^{-2}$ (s), an optimal state estimator and an optimal controller can be obtained by using the LQG methodology. This approach leads to the following set of discrete-time state-space and measurement equations:

$$\begin{cases} \hat{\mathbf{z}}(k+1) = \mathbf{A}\hat{\mathbf{z}}(k) + \mathbf{B}_e \mathbf{u}_e(k) + \mathbf{B}_c \mathbf{u}_c(k) \\ \quad + \mathbf{K}_\infty (\mathbf{y}(k) - \hat{\mathbf{y}}(k)) \\ \hat{\mathbf{y}}(k) = \mathbf{C}\hat{\mathbf{z}}(k) + \mathbf{D}_e \mathbf{u}_e(k) + \mathbf{D}_c \mathbf{u}_c(k) \\ \mathbf{u}_c(k) = \mathbf{F}_\infty \hat{\mathbf{z}}(k) \end{cases} \quad (59)$$

where k is the discrete time, $\hat{\mathbf{z}}(k)$ is the estimated discrete-time state vector, and $\hat{\mathbf{y}}(k)$ denotes the estimated discrete-time measurement vector. In these equations, the matrices \mathbf{K}_∞ and \mathbf{F}_∞ represent a discrete-time infinite-horizon Kalman filter gain and a discrete-time infinite-horizon optimal feedback gain, respectively, which can be readily computed by using the LQG regulation and estimation method. The discrete-time state-space model given by the set of matrices \mathbf{A} , \mathbf{B}_e , \mathbf{B}_c , \mathbf{C} , \mathbf{D}_e , and \mathbf{D}_c can be easily derived from the mechanical model of the two-story frame structure combined with the pendulum system. In order to analyze the dynamic behavior of the two-story structural system with and without the action of the feedback controller, the control input is deactivated in the time range between $t = 0$ (s) and $t = 32$ (s) and it is activated in the time range between $t = 32$ (s) and $t = 64$ (s). The estimated displacement of the first floor of the frame structure resulting from the implementation of the control system is shown in figure 9, whereas the corresponding control torque used as a controllable input signal is represented in figure 10. Observing the estimated displacement shown in figure 9, it is apparent that the action of the feedback controller allows for obtaining a considerable amplitude reduction of the system mechanical vibrations. The reduction of the system vibrations can be quantitatively

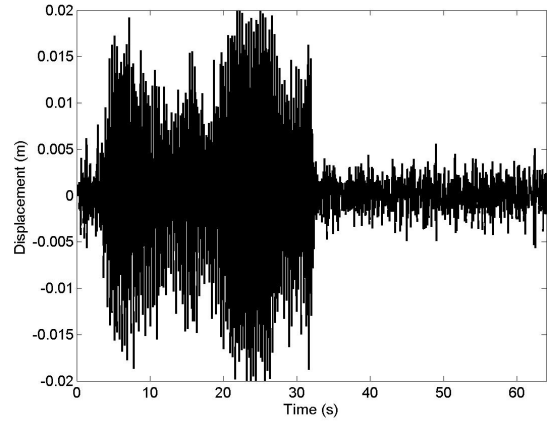


Fig. 9. Estimated displacement of the first floor

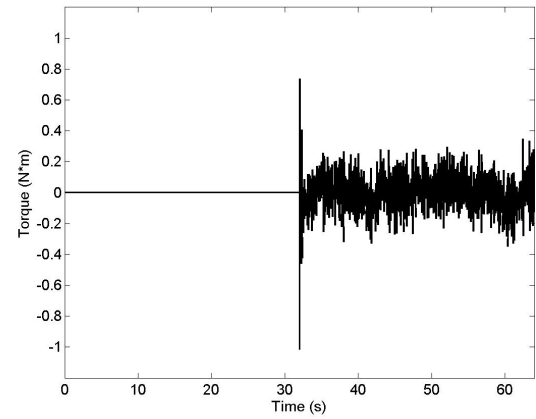


Fig. 10. Control torque

measured by comparing the maximum amplitude values of the system displacements with and without the action of the feedback controller. This quantitative comparison can be carried out as follows:

$$\begin{cases} (x_{1,\max}^{nc} - x_{1,\max}^c) / x_{1,\max}^{nc} = 76.93 (\%) \\ (x_{2,\max}^{nc} - x_{2,\max}^c) / x_{2,\max}^{nc} = 65.78 (\%) \end{cases} \quad (60)$$

where $x_{1,\max}^{nc}$ and $x_{2,\max}^{nc}$ denote the maximum values of the estimated structural displacements when there is no control action, whereas $x_{1,\max}^c$ and $x_{2,\max}^c$ represent the maximum values of the estimated structural displacements when the feedback controller acts on the pendulum attached on the two-story structure. It is important to note that the numerical results found in this section are consistent with the system actual dynamic behavior observed during the experimental testing.

VII. SUMMARY, CONCLUSIONS, AND FUTURE WORK

The main research areas of interest for the authors are multibody dynamics [58], [59], [60], [61], system identification [62], [63], [64], [65], and nonlinear control [66], [67], [68], [69], [70]. In this respect, the research of the authors is focused on the development of new methods for obtaining accurate analytic modeling [71], [72], [73], new numerical parameter identification methodologies based on experimental

data [74], [75], [76], and new control approaches suitable for regulating the dynamic behavior of rigid-flexible multibody systems [77], [78], [79], [80], [81], [82], [83], [84], [85], [86]. This paper, on the other hand, is concerned with the development of a time-domain system identification method for obtaining first-order state-space models and second-order mechanical models based on the system configuration space and using experimental input-output data. The case study considered for the experimental testing of the system identification numerical procedure developed in this work is a frame structure that can be modeled as a lumped parameter system. First, the frame structure is modeled as a two-story shear building system that is mathematically described by using a two-degree-of-freedom lumped parameter mechanical model. This simplified model is readily developed in the paper employing the analytical methods of classical mechanics. The natural frequencies and the mode shapes obtained analytically by using the preliminary mechanical model based on the lumped parameter approach are useful for guiding the experimental identification process and for assessing the quality of the numerical results obtained by using the proposed system identification approach. The proposed system identification numerical procedure is developed employing the combination of the Observer/Kalman Filter Identification Method (OKID) with the Eigensystem Realization Algorithm (ERA). The proposed methodology is used in this work for performing the experimental modal analysis of the two-story shear building system employing an impulsive excitation as the input force measurement and recording the corresponding structural accelerations as output measurements. In particular, the method developed in this paper leads to the identification of a first-order state-space model and to the reconstruction of a second-order mechanical model which can be readily performed in the time domain by using input force measurements and output acceleration measurements recorded from the vibrations of the frame structure. Subsequently, the first-order dynamical model of the mechanical system considered as the case study is used for performing the experimental modal analysis in order to obtain the system modal parameters. For this purpose, in order to obtain a reliable estimation of the system mass, stiffness, and damping matrices, a method for extracting a second-order mechanical model from an identified state-space realization is used. Furthermore, the estimation of the system damping is improved by using an approximation method based on the least-square computational approach and assuming the proportional damping hypothesis. Finally, the second-order mechanical model identified in this investigation is used for developing an actively controlled inertial-based vibration absorber based on the Linear Quadratic Gaussian (LQG) control and estimation approach. The actively controlled inertial-based vibration absorber is realized employing a physical pendulum hinged on the second floor of the frame structure. The pendulum system is controlled using a brushless motor and the feedback control action is computed in real time by using a digital controller. The numerical and experimental results shown in the paper confirmed the effectiveness of the methodology proposed in this investigation. However, the goal of the future research developments will be to obtain the suppression of the mechanical vibrations of three-dimensional frame structures that are induced by multiple

external sources of disturbances. Therefore, future research will be devoted to the analytical derivation, the practical implementation, and the experimental testing of more complex identification and control techniques.

REFERENCES

- [1] Ljung, L., 1999, System identification, John Wiley and Sons.
- [2] Ljung, L., 2010, "Perspectives on System Identification", Annual Reviews in Control, 34(1), pp. 1-12.
- [3] Sun, X., Li, Y., Liu, J., and Zhang, M., 2017, "Echo State Wavelet-sigmoid Networks and Their Application to Nonlinear System Identification", Engineering Letters, 25(3), pp. 301-311.
- [4] Jami'in, M. A., Yuyun, and Julianto, E., 2017, "Hierarchical Algorithms of Quasi-Linear ARX Neural Networks for Identification of Nonlinear Systems", Engineering Letters, 25(3), pp. 321-328.
- [5] Zheng, K., Zhang, Y., Xiao, H., Luo, J., Su, Z., and Ye, Z., 2016, "Crank Identification of the Rotary Kiln Based on WTD-EEMD Using Vibration Monitoring of the Supporting Rollers", Engineering Letters, 24(4), pp. 429-440.
- [6] Liu, H., and Li, Y., 2016, "Safety Evaluation of a Long-Span Steel Trestle with an Extended Service Term Age in a Coastal Port Based on Identification of Modal Parameters", Engineering Letters, 24(1), pp. 84-92.
- [7] Lazaro, I. I., Alvarez, A., and Anzurez, J., 2013, "The Identification Problem Applied to Periodic Systems Using Hartley Series, Engineering Letters", 21(1), pp. 36-43.
- [8] Nelles, O., 2013, Nonlinear System Identification: From Classical Approaches to Neural Networks and Fuzzy Models, Springer Science and Business Media.
- [9] Peeters, B., and De Roeck, G., 2001, "Stochastic System Identification for Operational Modal Analysis: a Review", Journal of Dynamic Systems, Measurement, and Control, 123(4), pp. 1-9.
- [10] Reynders, E., 2012, "System Identification Methods for (Operational) Modal Analysis: Review and Comparison", Archives of Computational Methods in Engineering, 19(1), pp. 51-124.
- [11] Wang, J. S., and Li, S. X., 2017, "PID Decoupling Controller Design for Electroslag Remelting Process Using Cuckoo Search Algorithm with Self-tuning Dynamic Searching Mechanism", Engineering Letters, 25(2), pp. 125-133.
- [12] Zhang, J., Yu, L., and Ding, L., 2016, "Velocity Feedback Control of Swing Phase for 2-DoF Robotic Leg Driven by Electro-hydraulic Servo System", Engineering Letters, 24(4), pp. 378-383.
- [13] Guo, Q. W., Song, W. D., Gao, M., and Fang, D., 2016, "Advanced Guidance Law Design for Trajectory-Corrected Rockets with Canards under Single Channel Control", Engineering Letters, 24(4), pp. 469-477.
- [14] Hong, X., Mitchell, R. J., Chen, S., Harris, C. J., Li, K., and Irwin, G. W., 2008, "Model Selection Approaches for Non-linear System Identification: a Review", International Journal of Systems Science, 39(10), pp. 925-946.
- [15] Unbehauen, H., and Rao, G. P., 1998, "A Review of Identification in Continuous-time Systems", Annual Reviews in Control, 22, pp. 145-171.
- [16] Tian, Z., Li, S., Wang, Y., and Gu, B., 2017, "Priority Scheduling of Networked Control System Based on Fuzzy Controller with Self-tuning Scale Factor", IAENG International Journal of Computer Science, 44(3), pp. 308-315.
- [17] El Kafhali, S., and Hanini, M., 2017, "Stochastic Modeling and Analysis of Feedback Control on the QoS VoIP Traffic in a single cell IEEE 802.16 e Networks", IAENG International Journal of Computer Science, 44(1), pp. 19-28.
- [18] Taniguchi, T., and Sugeno, M., 2017, "Trajectory Tracking Controls for Non-holonomic Systems Using Dynamic Feedback Linearization Based on Piecewise Multi-Linear Models", IAENG International Journal of Applied Mathematics, 47(3), pp. 339-351.
- [19] Zhang, X., and Yuan, D., 2017, "A Niche Ant Colony Algorithm for Parameter Identification of Space Fractional Order Diffusion Equation", IAENG International Journal of Applied Mathematics, 47(2), pp. 197-208.
- [20] Juang, J. N., and Phan, M. Q., 2001, Identification and Control of Mechanical Systems, Cambridge University Press.
- [21] Katayama, T., 2006, Subspace Methods for System Identification, Springer Science and Business Media.
- [22] Shamshiri, R., Ismail, W. I. W., and Moradi, M., 2012, "Full-state Feedback Controller for a Tractor Active Suspension", In International Conference on Agricultural and Food Engineering for Life, Cafei2012, 26, pp. 28.

- [23] Colombo, F., Moradi, M., Raparelli, T., Trivella, A., and Viktorov, V., 2017, "Dynamic Lumped Model of an Externally Pressurized Air Bearing", Programme and Proceedings of AIMETA 2017, XXIII Conference, Salerno, Italy, September 4-7.
- [24] Ruggiero, A., Affatato, S., Merola, M., and De Simone, M. C., 2017, "FEM Analysis of Metal on UHMWPE Total Hip Prosthesis During Normal Walking Cycle", Programme and Proceedings of AIMETA 2017, XXIII Conference, Salerno, Italy, September 4-7.
- [25] De Simone, M. C., Guida, D., 2017, "On the Development of a Low Cost Device for Retrofitting Tracked Vehicles for Autonomous Navigation", Programme and Proceedings of AIMETA 2017, XXIII Conference, Salerno, Italy, September 4-7.
- [26] Villecco, F., and Pellegrino, A., 2017, "Evaluation of Uncertainties in the Design Process of Complex Mechanical Systems", *Entropy*, 19(9), 475.
- [27] Villecco, F., and Pellegrino, A., 2017, "Entropic Measure of Epistemic Uncertainties in Multibody System Models by Axiomatic Design", *Entropy*, 19(7), 291.
- [28] Mercere, G., Markovsky, I., and Ramos, J. A., 2016, "Innovation-based Subspace Identification in Open-and Closed-loop", *IEEE 55th Conference on Decision and Control (CDC)*, pp. 2951-2956.
- [29] Alenany, A., Mercere, G., and Ramos, J. A., 2017, "Subspace Identification of 2-D CRSD Roesser Models With Deterministic-Stochastic Inputs: A State Computation Approach", *IEEE Transactions on Control Systems Technology*, 25(3), pp. 1108-1115.
- [30] Ramos, J. A., and Mercere, G., 2016, "Subspace Algorithms for Identifying Separable-in-denominator 2D Systems with Deterministic-stochastic Inputs", *International Journal of Control*, 89(12), pp. 2584-2610.
- [31] Prot, O., Mercere, G., and Ramos, J., 2012, "A Null-space-based Technique for the Estimation of Linear-time Invariant Structured state-space Representations", *IFAC Proceedings Volumes*, 45(16), pp. 191-196.
- [32] Dos Santos, P. L., Ramos, J. A., Azevedo-Perdicoulis, T. P., and De Carvalho, J. M., 2015, "Deriving Mechanical Structures in Physical Coordinates from Data-driven State-space Realizations", *IEEE American Control Conference (ACC)*, pp. 1107-1112.
- [33] Mercere, G., Prot, O., and Ramos, J. A., 2014, "Identification of Parameterized Gray-box State-space Systems: From a Black-box Linear Time-invariant Representation to a Structured One", *IEEE Transactions on Automatic Control*, 59(11), pp. 2873-2885.
- [34] De Simone, M. C., and Guida, D., 2015, "Dry friction influence on structure dynamics", *COMPADYN 2015 - 5th ECCOMAS Thematic Conference on Computational Methods in Structural Dynamics and Earthquake Engineering*, pp. 4483-4491.
- [35] Ruggiero, A., De Simone, M. C., Russo, D., and Guida D., 2016, "Sound pressure measurement of orchestral instruments in the concert hall of a public school", *International Journal of Circuits, Systems and Signal Processing*, 10, pp. 75-812.
- [36] De Simone, M. C., Russo, S., Rivera, Z. B., and Guida, D., 2017, "Multibody Model of a UAV in Presence of Wind Fields", *ICCAIRO 2017: International Conference on Control, Artificial Intelligence, Robotics and Optimization*, Prague, Czech Republic, May 20-22, 2017.
- [37] De Simone, M. C., Rivera, Z. B., and Guida, D., 2017, "A New Semi-Active Suspension System for Racing Vehicles", *FME Transactions*, 45(4), pp. 579.
- [38] Quatrano, A., De Simone, M. C., Rivera, Z. B., and Guida, D., 2017, "Development and Implementation of a Control System for a Retrofitted CNC Machine by Using Arduino", *FME Transactions*, 45, pp. 578-584.
- [39] Nagarkar, M. P., Patil, G. J. V., and Patil, R. N. Z., 2016, "Optimization of Nonlinear Quarter Car Suspension-seat-driver Model", *Journal of Advanced Research*, 7(6), pp. 991-1007.
- [40] Nagarkar, M. P., and Patil, V. G., 2016, "Multi-objective Optimization of LQR Control Quarter Car Suspension System using Genetic Algorithm", *FME Transactions*, 44(2), pp. 187-196.
- [41] Borozan, I., Cosco, F., and Argesanu, V., 2015, "Improving Driver Comfort with Linear Quadratic Controller for Active Suspension System", *Applied Mechanics and Materials*, 811, pp. 199-203.
- [42] Carpinelli, M., Gubitosa, M., Mundo, D., and Desmet, W., 2013, "Parameters Identification Strategy for a Generalized Vehicle Concept Model for Ride and Handling Analysis", *ASME 2013 International Design Engineering Technical Conferences and Computers and Information in Engineering Conference*, pp. V001T01A021-V001T01A021.
- [43] Thothadri, M., Casas, R. A., Moon, F. C., D'Andrea, R., and Johnson, C. R., 2003, "Nonlinear System Identification of Multi-degree-of-freedom Systems", *Nonlinear Dynamics*, 32(3), pp. 307-322.
- [44] Hou, Z. Q., and Lucifredi, A., 1995, "On the use of Neural Networks for Identification of Linear and Nonlinear Systems", *Meccanica*, 30(4), pp. 377-388.
- [45] Rudinger, F., and Krenk, S., 2004, "Identification of Nonlinear Oscillator with Parametric White Noise Excitation", *Nonlinear Dynamics*, 36(2-4), pp. 379-403.
- [46] Ikonen, E., and Najim, K., 2001, *Advanced Process Identification and Control*, CRC Press.
- [47] Liu, T., and Gao, F., 2011, *Industrial Process Identification and Control Design: Step-test and Relay-experiment-based Methods*, Springer Science and Business.
- [48] Stengel, R. F., 2012, *Optimal Control and Estimation*, Courier Corporation.
- [49] Da Conceicao, S. M., Vasques, C. H., De Abreu, G. L. C. M., Lopes Jr, V., and Brennan, M. J., 2014, "Experimental Identification and Control of a Cantilever Beam Using ERA/OKID with a LQR Controller", *Journal of Control, Automation and Electrical Systems*, 25(2), pp. 161-173.
- [50] Juang, J. N., Phan, M., Horta, L. G., and Longman, R. W., 1993, "Identification of Observer/Kalman Filter Markov Parameters - Theory and Experiments", *Journal of Guidance, Control, and Dynamics*, 16(2), pp. 320-329.
- [51] Phan, M., Horta, L., Juang, J. N., and Longman, R. W., 1995, "Improvement of Observer/Kalman Filter Identification (OKID) by Residual Whitening", *Conference on Guidance, Navigation and Control*, p. 4385.
- [52] Juang, J. N., and Pappa, R. S., 1985, "An Eigensystem Realization Algorithm for Modal Parameter Identification and Model Reduction", *Journal of Guidance, Control, and Dynamics*, 8(5), pp. 620-627.
- [53] Juang, J. N., and Pappa, R. S., 1986, "Effects of noise on modal parameters identified by the eigensystem realization algorithm", *Journal of Guidance, Control, and Dynamics*, 9(3), pp. 294-303.
- [54] Lus, H., Betti, R., Yu, J., and De Angelis, M., 2004, "Investigation of a System Identification Methodology in the context of the ASCE Benchmark Problem", *Journal of Engineering Mechanics*, 130(1), pp. 71-84.
- [55] Lus, H., De Angelis, M., Betti, R., Longman, R. W., 2003, "Constructing Second-order Models of Mechanical Systems from Identified State Space Realizations. Part I: Theoretical discussions", *Journal of Engineering Mechanics*, 129(5), pp. 477-488.
- [56] Lus, H., De Angelis, M., Betti, R., and Longman, R. W., 2003, "Constructing Second-order Models of Mechanical Systems from Identified State space Realizations. Part II: Numerical Investigations", *Journal of Engineering Mechanics*, 129(5), pp. 489-531.
- [57] Gawronski, W., 2004, *Advanced Structural Dynamics and Active Control of Structures*, Springer Science and Business Media.
- [58] Pappalardo, C. M., 2014, "Modelling Rigid Multibody Systems using Natural Absolute Coordinates", *Journal of Mechanical Engineering and Industrial Design*, 3(1), pp. 24-38.
- [59] Pappalardo, C. M., 2015, "A Natural Absolute Coordinate Formulation for the Kinematic and Dynamic Analysis of Rigid Multibody Systems", *Nonlinear Dynamics*, 81(4), pp. 1841-1869.
- [60] Pappalardo, C. M., Wallin, M., and Shabana, A. A., 2017, "A New ANCF/CRBF Fully Parametrized Plate Finite Element", *ASME Journal of Computational and Nonlinear Dynamics*, 12(3), pp. 1-13.
- [61] Pappalardo, C. M., Yu, Z., Zhang, X., and Shabana, A. A., 2016, "Rational ANCF Thin Plate Finite Element", *ASME Journal of Computational and Nonlinear Dynamics*, 11(5), pp. 1-15.
- [62] Guida, D., Nilvetti, F., and Pappalardo, C. M., 2009, "Parameter Identification of a Two Degrees of Freedom Mechanical System", *International Journal of Mechanics*, 3(2), pp. 23-30.
- [63] Guida, D., Nilvetti, F., and Pappalardo, C. M., 2009, "On Parameter Identification of Linear Mechanical Systems", *Programme and Proceedings of 3rd International Conference on Applied Mathematics, Simulation, Modelling (ASM'09)*, Vouliagmeni Beach, Athens, Greece, December 29-31, pp. 55-60.
- [64] Guida, D., and Pappalardo, C. M., 2009, "Sommerfeld and Mass Parameter Identification of Lubricated Journal Bearing", *WSEAS Transactions on Applied and Theoretical Mechanics*, 4(4), pp. 205-214.
- [65] Guida, D., Nilvetti, F., and Pappalardo, C. M., 2011, "Mass, Stiffness and Damping Identification of a Two-story Building Model", *Programme and Proceedings of rd ECCOMAS Thematic Conference on Computational Methods in Structural Dynamics and Earthquake Engineering (COMPADYN 2011)*, Corfu, Greece, May 25-28, pp. 25-28.
- [66] Pappalardo, C. M., Patel, M., Tinsley, B., and Shabana, A. A., 2015, "Pantograph/Catenary Contact Force Control", *Proceedings of the ASME 2015 International Design Engineering Technical Conferences and Computers and Information in Engineering Conference IDETC/CIE 2015*, Boston, Massachusetts, USA, August 2-5, pp. 1-11.
- [67] Pappalardo, C. M., Patel, M. D., Tinsley, B., and Shabana, A. A., 2016, "Contact Force Control in Multibody Pantograph/Catenary Systems",

- Proceedings of the Institution of Mechanical Engineers, Part K: Journal of Multibody Dynamics, 230(4), pp. 307-328.
- [68] Guida, D., and Pappalardo, C. M., 2015, "Control Design of an Active Suspension System for a Quarter-Car Model with Hysteresis", Journal of Vibration Engineering and Technologies, 3(3), pp. 277-299.
- [69] Guida, D., Nilvetti, F., and Pappalardo, C. M., 2013, "Optimal Control Design by Adjoint-Based Optimization for Active Mass Damper with Dry Friction", Programme and Proceedings of COMPDYN 2013 4th International Conference on Computational Methods in Structural Dynamics and Earthquake Engineering, Kos Island, Greece, June 12-14, pp. 1-19.
- [70] Guida, D., Nilvetti, F., and Pappalardo, C. M., 2009, "Instability Induced by Dry Friction", International Journal of Mechanics, 3(3), pp. 44-51.
- [71] Pappalardo, C. M., Wang, T., and Shabana, A. A., 2017, "On the Formulation of the Planar ANCF Triangular Finite Elements", Nonlinear Dynamics, 89(2), pp. 1019-1045.
- [72] Guida, D., Nilvetti, F., and Pappalardo, C. M., 2009, "Dry Friction Influence on Cart Pendulum Dynamics", International Journal of Mechanics, 3(2), pp. 31-38.
- [73] Guida, D., Nilvetti, F., and Pappalardo, C. M., 2009, "Dry Friction Influence on Inverted Pendulum Control", Programme and Proceedings of 3rd International Conference on Applied Mathematics, Simulation, Modelling (ASM'09), Vouliagmeni Beach, Athens, Greece, December 29-31, pp. 49-54.
- [74] Guida, D., Nilvetti, F., and Pappalardo, C. M., 2011, "Experimental Investigation On a New Hybrid Mass Damper", Programme and Proceedings of 8th International Conference on Structural Dynamics (EURODYN 2011), Leuven, Belgium, July 4-6, pp. 1644-1649.
- [75] Guida, D., Nilvetti, F., and Pappalardo, C. M., 2010, "Friction Induced Vibrations of a Two Degrees of Freedom System", Programme and Proceedings of 10th WSEAS International Conference on Robotics, Control and Manufacturing Technology (ROCOM '10), Hangzhou, China, April 11-13, pp. 133-136.
- [76] Guida, D., Nilvetti, F., and Pappalardo, C. M., 2013, "Adjoint-based Optimal Control Design for a Cart Pendulum System with Dry Friction", Programme and Proceedings of ECCOMAS Thematic Conference on Multibody Dynamics, Zagreb, Croatia, July 1-4, pp. 269-285.
- [77] Guida, D., and Pappalardo, C. M., 2013, "A New Control Algorithm for Active Suspension Systems Featuring Hysteresis", FME Transactions, 41(4), pp. 285-290.
- [78] Guida, D., and Pappalardo, C. M., 2014, "Forward and Inverse Dynamics of Nonholonomic Mechanical Systems", Meccanica, 49(7), pp. 1547-1559.
- [79] Pappalardo, C. M., and Guida, D., 2016, "Control of Nonlinear Vibrations using the Adjoint Method", Meccanica, 52(11-12), pp. 2503-2526.
- [80] Pappalardo, C. M., and Guida, D., 2017, "Adjoint-based Optimization Procedure for Active Vibration Control of Nonlinear Mechanical Systems", ASME Journal of Dynamic Systems, Measurement, and Control, 139(8), 081010, pp. 1-11.
- [81] Pappalardo, C. M., Wang, T., and Shabana, A. A., 2017, "Development of ANCF Tetrahedral Finite Elements for the Nonlinear Dynamics of Flexible Structures", Nonlinear Dynamics, 89(4), pp. 2905-2932.
- [82] Pappalardo, C. M., and Guida, D., 2017, "On the use of Two-dimensional Euler Parameters for the Dynamic Simulation of Planar Rigid Multibody Systems", Archive of Applied Mechanics, 87(10), pp. 1647-1665.
- [83] Pappalardo, C. M., and Guida, D., 2017, "Comparative Analysis of Formulation Strategies and Solution Procedures for the Equations of Motion of Rigid Multibody Systems", Programme and Proceedings of AIMETA 2017, XXIII Conference, Salerno, Italy, September 4-7.
- [84] Pappalardo, C. M., and Guida, D., 2017, "Experimental Identification and Control of a Frame Structure using an Actively Controlled Inertial-based Vibration Absorber", Programme and Proceedings of the ICCAIRO 2017: International Conference on Control, Artificial Intelligence, Robotics, and Optimization, Prague, Czech Republic, May 20-22.
- [85] Pappalardo, C. M., and Guida, D., 2017, "On the Lagrange Multipliers of the Intrinsic Constraint Equations of Rigid Multibody Mechanical Systems", Archive of Applied Mechanics, Accepted for publication.
- [86] Kulkarni, S., Pappalardo, C. M., and Shabana, A. A., 2017, "Pantograph/Catenary Contact Formulations", ASME Journal of Vibrations and Acoustics, 139(1), 011010, pp. 1-12.



Carmine Maria Pappalardo received his B.S., M.S., and Ph.D. degrees with Summa Cum Laude honors in mechanical engineering from the University of Salerno, Fisciano, Italy, in 2006, 2008, and 2012, respectively. He was a Post-Doctorate at the Department of Industrial Engineering of the University of Salerno, Fisciano, Italy, from 2012 to 2014. He was a Visiting Researcher at the Department of Mechanical and Industrial Engineering of the University of Illinois at Chicago, Chicago, Illinois, United States, from 2014 to 2016. Since 2016, he is a Post-Doctorate at the Department of Industrial Engineering of the University of Salerno, Fisciano, Italy. His current research interests are multibody dynamics, nonlinear control, and system identification.



Domenico Guida received his M.S. degree with Cum Laude honors in mechanical engineering from the University of Naples "Federico II", Naples, Italy, in 1987. He received his Ph.D. degree in tribology from the University of Pisa, Pisa, Italy, in 1991. He was a Post-Doctorate at the Department of Mechanical Engineering of the University of Naples "Federico II", Naples, Italy, from 1991 to 1993. He was an Assistant Professor at the Department of Mechanical Engineering of the University of Naples "Federico II", Naples, Italy, from 1993 to 1996. He was an Associate Professor at the Department of Mechanical Engineering of the University of Salerno, Fisciano, Italy, from 1996 to 2000. Since 2000, he is Full Professor at the Department of Industrial Engineering of the University of Salerno, Fisciano, Italy. His current research interests are multibody dynamics, nonlinear control, and system identification.